Synchronization of noise-induced escape: how it starts and ends

M.I. Dykman and D. Ryvkine

Michigan State University, East Lansing, MI 48824, USA

ABSTRACT

We provide a complete solution of the problem of noise-induced escape in periodically driven systems. We show that both the exponent and the prefactor in the escape rate display scaling behavior with the field intensity. The corresponding scaling is related to synchronization of escape events by the modulating field. The onset of the synchronization with the increasing field and its loss as the field approaches a bifurcational value lead to a strongly nonmonotonic field dependence of the prefactor.

Keywords: Activated escape, driven systems, prefactor, scaling

1. INTRODUCTION

Thermally activated escape from a metastable state is often investigated in systems driven by time-dependent fields. Recent examples are activated transitions in modulated nanomagnets[1–3] and Josephson junctions.[4–6] Modulation changes the activation barrier. This enables efficient control of the escape rate and accurate measurement of the system parameters.[7,8] It also provides an insight into the dynamics of a system far away from its metastable states. Most frequently used types of modulation are slow ramping of a control parameter, when the system remains quasistationary, and periodic modulation. In the latter case the system is away from thermal equilibrium, which complicates the theoretical formulation of the escape problem.[9]

In the present paper[10] we extend to periodically modulated systems the analysis of the escape rate done by Kramers for systems in thermal equilibrium.[11] Our approach gives the full time-dependent escape rate $W(t)$ as well as the period-averaged rate $\overline{W} = \nu \exp(-R/D)$, where R is the activation energy of escape and D is the noise intensity, $D = k_B T$ for thermal noise. We show that the escape probability may display exponentially sharp periodic peaks as a function of time, which means that it is exponentially strongly synchronized by periodic modulation. Such synchronization occurs for comparatively low modulation frequency and exists in a limited range of modulation amplitudes. Our analysis allows us to study not only how it starts, but also how it ends with the increasing amplitude.

For comparatively small modulation amplitude A escape of a periodically driven Brownian particle was studied by Smelyanskiy *et al.*[12] The range of intermediate A and intermediate modulation frequencies ω_F was analyzed by Lehmann *et al.*[13] and by Maier and Stein.[14] Here we find $W(t)$ for an arbitrary A and an arbitrary interrelation between ω_F and the relaxation time of the system t_r. We show that the prefactor ν depends on A strongly and nonmonotonically. It displays scaling behavior near the bifurcational modulation amplitude A_c where the metastable state disappears.

In the spirit of Kramers' approach, we relate the instantaneous escape rate $W(t)$ to the current *well behind* the boundary $q_b(t)$ of the basin of attraction to the initially occupied metastable state (q is the system coordinate). This is the current usually studied in experiments. Because of the oscillations of $q_b(t)$, it has a different functional form from the current[13,14] at the basin boundary $q_b(t)$.

We find $W(t)$ by matching the boundary-layer probability distribution near $q_b(t)$ with the distribution $\rho(q,t)$ well inside the basin of attraction. The boundary-layer distribution is obtained by linearizing the equation of motion near $q_b(t)$, whereas the distribution inside the basin is obtained using the eikonal approximation. Quite remarkably, for sufficiently strong modulation the matching of the two distributions can be done without full determination of all parameters of $\rho(q,t)$ near $q_b(t)$, using singular features of the dynamics of large fluctuations.

Send correspondence to dykman@pa.msu.edu

2. THE FOKKER-PLANCK EQUATION

We consider noise-induced escape of a periodically modulated overdamped Brownian particle. The probability distribution of such particle $\rho(q,t)$ is given by the solution of the Fokker-Planck equation (FPE)

$$\partial_t \rho = -\partial_q \left[K(q,t)\rho \right] + D\partial_q^2 \rho. \tag{1}$$

Here, $K(q,t)$ is the periodic force driving the particle, $K(q,t) = K(q,t+\tau_F) \equiv -\partial_q U(q,t)$, where $\tau_F = 2\pi/\omega_F$ is the modulation period and $U(q,t)$ is the metastable potential. The metastable state $q_a(t)$, from the vicinity of which the system escapes due to noise, and the basin boundary $q_b(t)$ are, respectively, the stable and unstable periodic solutions of the equation of motion of the particle in the absence of noise,

$$\dot{q}_i = K(q_i, t), \qquad q_i(t+\tau_F) = q_i(t) \qquad (i = a, b). \tag{2}$$

We will assume that the noise intensity D is small. Then in a broad time range $t_{\rm r} \ll t \ll 1/\overline{W}$ the distribution $\rho(q,t)$ is nearly periodic in the basin of attraction to $q_a(t)$. The current away from this basin, and thus the escape rate $W(t)$, are also periodic.

The distribution ρ is maximal at the metastable stable state $q_a(t)$ and falls off exponentially away from it. In the presence of periodic driving it acquires singular features as $D \to 0$,[15] some of which have counterparts in wave fields,[16] with D playing the role of the wavelength. The singularities accumulate near $q_b(t)$. In order to find $W(t)$ one has to understand how they are smeared by diffusion.

In the absence of noise the motion of the system close to the periodic states $q_i(t)$ $(i = a, b)$ is described by the equation $\dot{q} = K$ with K linearized in $q - q_i(t)$. The evolution of $q(t) - q_i(t)$ is given by the factors

$$\kappa_i(t,t') = \exp\left[\int_{t'}^{t} d\tau\, \mu_i(\tau) \right] \quad (i = a, b), \tag{3}$$

where $\mu_i(t) = \mu_i(t+\tau_F) \equiv [\partial_q K(q,t)]_{q_i(t)}$. Over the period τ_F the distance $q(t) - q_i(t)$ decreases (for $i = a$) or increases (for $i = b$) by the Floquet multiplier $M_i = \kappa_i(t+\tau_F, t) \equiv \exp(\bar{\mu}_i \tau_F)$, where $\bar{\mu}_i$ is the period-average value of $\mu_i(t)$, with $\bar{\mu}_a < 0, \bar{\mu}_b > 0$.

For weak noise the expansions of K can be used to find $\rho(q,t)$ near $q_{a,b}(t)$. Near the metastable state q_a, the distribution ρ is Gaussian,[17] $\rho(q,t) \propto \exp\{-[q - q_a(t)]^2/2D\sigma_a^2(t)\}$. The reduced time-periodic variance is given by the equation

$$\sigma_i^2(t) = 2 \left| M_i^{-2} - 1 \right|^{-1} \int_0^{\tau_F} dt_1 \kappa_i^{-2}(t+t_1, t) \tag{4}$$

with $i = a$ (in the absence of modulation $\sigma_a^2 = 1/|\mu_a|$).

2.1. The boundary-layer distribution

The general form of the periodic distribution near the unstable state $q_b(t)$ (the boundary-layer distribution) can be found from Eq. (1) using the Laplace transform, similar to the weak-driving limit.[12] With K linear in $q - q_b$, the equation for the Laplace transform of $\rho(q,t)$ is of the first order, giving

$$\begin{aligned}
\rho(q,t) &= \int_0^{\infty} dp\, e^{-pQ/D}\, \tilde{\rho}(p,t),\ Q = q - q_b(t), \\
\tilde{\rho}(p,t) &= \mathcal{E}D^{-1/2} \exp\left\{ -\left[s(\phi) + p^2 \sigma_b^2(t)/2 \right] /D \right\}.
\end{aligned} \tag{5}$$

In Eq. (5), $\mathcal{E}$ is a constant, $s(\phi)$ is an arbitrary zero-mean periodic function, $s(\phi + 2\pi) = s(\phi)$, and $\phi \equiv \phi(p,t)$,

$$\phi(p,t) = \Omega_F \ln[p\,\kappa_b(t,t')/\bar{\mu}_b l_D]. \tag{6}$$

Here, $\Omega_F = \omega_F/\bar{\mu}_b \equiv 2\pi/\ln M_b$ is the reduced field frequency, $l_D = (2D/\bar{\mu}_b)^{1/2}$ is the typical diffusion length, and t' determines the initial value of ϕ; from Eq. (6), $\phi(p, t+\tau_F) = \phi(p,t) + 2\pi$. In Eq. (5) we assumed that the basin of attraction to q_a lies for $q < q_b(t)$, and $|Q| \ll \Delta q \equiv \min_t[q_b(t) - q_a(t)]$ (Δq characterizes the distance between the stable and unstable states of the system).

3. GENERAL EXPRESSION FOR THE ESCAPE RATE

The form (5) is advantageous as it immediately gives the current $j(q,t)$ from the occupied region $(-\infty, q]$. Well behind the basin boundary, where $Q = q - q_b(t) \gg l_D$, diffusion can be disregarded. In this range the current is convective. It gives the instantaneous escape rate, and we will call it escape current. With $\dot{q} \approx \dot{q}_b + \mu_b Q$ in the absence of noise, we have $j(q,t) \approx \mu_b(t)\rho(q,t)Q$ at a given distance Q from $q_b(t)$. Disregarding the term $\propto p^2/D$ in $\tilde{\rho}$ for $Q \gg l_D$, we obtain from Eq. (5)

$$j(q,t) = \mu_b(t)\mathcal{E}D^{1/2} \int_0^\infty dx\, e^{-x} \exp[-s(\phi_d)/D]. \tag{7}$$

Here, ϕ_d and $t_d \equiv t_d(Q,t)$ are given by the equations

$$\phi_d = \Omega_F \ln[x\,\kappa_b(t_d,t')], \qquad \kappa_b(t_d,t) = l_D/2Q. \tag{8}$$

In the whole harmonic range j depends on the observation point Q only in terms of the delay time t_d, which shows how long it took the system to roll down to the point Q, $\partial t_d/\partial Q = -1/\mu_b(t_d)Q$. We note that $\mu_b(t)$ can be negative for a part of the period, leading to reversals of the instantaneous current.

The escape rate $\overline{W}$ is given by the period-averaged escape current $j(q,t)$ and is independent of q. From Eq. (7)

$$\overline{W} = \frac{\bar{\mu}_b}{2\pi}\mathcal{E}D^{1/2} \int_0^{2\pi} d\phi\, \exp[-s(\phi)/D]. \tag{9}$$

Eqs. (7) and (9) provide a complete solution of the Kramers problem of escape of a modulated system and reduce it to finding the function s. They are similar in form to the expressions for the instantaneous and average escape rates for comparatively weak modulation, $|s| \ll R$, where s was obtained explicitly.[12]

Unless the modulation is very weak or has a high frequency, for small noise intensity $\max s \sim |\min s| \gg D$. In this case the major contribution to the integrals in Eqs. (7), (9) comes from the range where s is close to its minimum s_m reached for some $\phi = \phi_m$. Then the escape current $j(q,t)$ sharply peaks as function of time once per period when $\phi_d \equiv \phi_d(t) = \phi_m$. This means that escape events are *strongly synchronized*. As we show, both $j(q,t)$ and $\overline{W}$ are determined not by the global shape of $s(\phi)$, but only by the curvature of $s(\phi)$ near ϕ_m.

4. DISTRIBUTION MATCHING

4.1. Intrawell distribution

To find $j(q,t)$ we match Eq. (5) to the distribution $\rho(q,t)$ close to $q_b(t)$ but well inside the attraction basin, $-Q \gg l_D$. For small D this distribution can be found, for example, by solving the FPE (1) in the eikonal approximation, $\rho(q,t) = \exp[-S(q,t)/D]$. To zeroth order in D, the equation for $S = S_0$ has the form of the Hamilton-Jacobi equation $\partial_t S_0 = -H$ for an auxiliary nondissipative system with the Hamiltonian[18]

$$H(q,p;t) = p^2 + pK(q,t), \; p = \partial_q S_0. \tag{10}$$

The Hamiltonian trajectories $q(t), p(t)$ of interest for the problem of fluctuations away from the metastable state $q_a(t)$ start in the vicinity of this state. The initial conditions follow from the Gaussian form of $\rho(q,t)$ near $q_a(t)$, with $S_0 = [q - q_a(t)]^2/2\sigma_a^2(t)$.

To logarithmic accuracy, the escape rate is determined by the probability to reach the basin boundary $q_b(t)$, i.e., by the action[9] $S_0(q_b(t),t)$. The Hamiltonian trajectory $q_{\mathrm{opt}}(t), p_{\mathrm{opt}}(t)$, which minimizes $S_0(q_b(t),t)$, approaches $q_b(t)$ asymptotically as $t \to \infty$. This is a heteroclinic trajectory of the auxiliary Hamiltonian system, it is periodically repeated in time with period τ_F. The coordinate along this trajectory $q_{\mathrm{opt}}(t)$ is the most probable escape path (MPEP) of the original system.

Close to $q_b(t)$, the Hamiltonian equations for $q(t), p(t)$ can be linearized and solved. On the MPEP

$$p_{\mathrm{opt}}(t) = -Q_{\mathrm{opt}}(t)/\sigma_b^2(t) = \kappa_b^{-1}(t,t')p_{\mathrm{opt}}(t'), \tag{11}$$
$$S_0(q_{\mathrm{opt}}(t),t) = R - Q_{\mathrm{opt}}^2(t)/2\sigma_b^2(t),$$

where $Q_{\mathrm{opt}}(t) = q_{\mathrm{opt}}(t) - q_b(t)$. The quantity $R = S_0\big(q_{\mathrm{opt}}(t), t\big)_{t\to\infty}$ is the activation energy of escape.

The surface $S_0(q,t)$ is flat[15] for small $Q - Q_{\mathrm{opt}}$. This is a consequence of nonintegrability of the dynamics with Hamiltonian (10). The action surface touches the surface $S_b(q,t) = R - Q^2/2\sigma_b^2(t)$ on the MPEP, $Q = Q_{\mathrm{opt}}(t)$. Away from the MPEP $S_0(q,t) > S_b(q,t)$, and therefore the function $\rho_b(q,t) = \rho(q,t)\exp[S_b(q,t)/D]$ is maximal on the MPEP.

4.2. Matching the exponents and the prefactors

We match on the MPEP ρ_b found in the eikonal approximation to the maximum of ρ_b found from Eq. (5) near the basin boundary. For $|s_{\mathrm{m}}| \gg D$ and $-Q \gg l_D$, the integral over p in Eq. (5) can be evaluated by the steepest descent method. The integrand is maximal if $p = -Q/\sigma_b^2(t)$ and s is minimal for this p, i.e., $\phi(p,t) = \phi_{\mathrm{m}}$ and $s = s_{\mathrm{m}}$. If the extremum lies on the MPEP for one time, $s = s_{\mathrm{m}}$ for all times, because $\phi(p_{\mathrm{opt}}(t), t) = $const. Then from Eq. (5)

$$\rho(q,t) = \mathcal{E}_b(t)\exp[-S_b(q,t)/D],$$
$$\mathcal{E}_b(t) = \tilde{\mathcal{E}} D^{-1/2}\left[\sigma_b^2(t) + \Omega_F^2\, s_{\mathrm{m}}''\, p_{\mathrm{opt}}^{-2}(t)\right]^{-1/2}, \tag{12}$$

where $\tilde{\mathcal{E}} = \mathcal{E}(2\pi D)^{1/2}\exp[(R - s_{\mathrm{m}})/D]$, and $s_{\mathrm{m}}'' \equiv [d^2s/d\phi^2]_{\phi_{\mathrm{m}}}$. From Eqs. (11), (12), not only the exponents, but also their slopes coincide along the MPEP for the boundary-layer and eikonal-approximation distributions.

The function $\mathcal{E}_b(t)$ should match on the MPEP the prefactor of the eikonal-approximation distribution $\rho = \exp(-S/D)$, which is given by the term $S_1 \propto D$ in S. On the MPEP, $z = \exp(2S_1/D)$ obeys the equation[19]

$$d^2z/dt^2 - 2d(z\,\partial_q K)/dt + 2zp\partial_q^2 K = 0, \tag{13}$$

where $q = q_{\mathrm{opt}}(t)$, $p = p_{\mathrm{opt}}(t)$. The initial condition to this equation follows from $\rho(q,t) = z^{-1/2}\exp(-S_0/D)$ being Gaussian near $q_a(t)$, which gives $z(t) \to 2\pi D\sigma_a^2(t)$ for $t \to -\infty$. Close to $q_b(t)$, from Eq. (13) $z(t) = D[z_1\sigma_b^2(t) + z_2 p_{\mathrm{opt}}^{-2}(t)]$, where $z_{1,2}$ are constants.[13] We note that the term $\propto z_1$ was disregarded by Lehmann et al[13] .

Remarkably, $z^{-1/2}(t)$ is of the same functional form near $q_b(t)$ as $\mathcal{E}_b(t)$ in Eq. (12). Thus, with an appropriate choice of constants $\mathcal{E}, s_{\mathrm{m}}''$ the prefactors in $\rho(q,t)$ as given by the eikonal and the boundary-layer approximations match each other.

5. INSTANTANEOUS ESCAPE RATE

Explicit expressions for the escape rate in the regime of strong synchronization can be obtained for comparatively weak or slow modulation, where $s_{\mathrm{m}}'' \sim |s_{\mathrm{m}}| \gg D$ but

$$\Omega_F^2 s_{\mathrm{m}}'' \ll R. \tag{14}$$

The results for $D \ll |s_{\mathrm{m}}| \ll R$ should coincide with the results[12] for moderately weak driving, which were obtained in a different way. We have verified this by finding s_{m}'' from Eq. (13) by perturbation theory in the modulation amplitude A.

5.1. Adiabatic regime

Condition (14) can be met for large A, where $s_{\mathrm{m}}'' \sim R$, provided the modulation frequency is small, $\omega_F t_{\mathrm{r}} \sim \Omega_F \ll 1$ (adiabatic modulation). Here, the MPEP is given by the equation $\dot{q}_{\mathrm{opt}} = -K\big(q_{\mathrm{opt}}, t_{\mathrm{m}}\big)$, with t_{m} found from the condition of the minimum of the adiabatic barrier height $\Delta U(t) = U\big(q_b(t), t\big) - U\big(q_a(t), t\big)$. The activation energy $R = \Delta U_{\mathrm{m}} \equiv \Delta U(t_{\mathrm{m}})$.

The value of s_{m}'' can be obtained from $z(t)$ or by matching the adiabatic intrawell distribution $\propto \exp[-U(q,t)/D]$ and the boundary layer distribution (5) in the region $|Q| \gg l_D$ and $\Omega_F^2 s_{\mathrm{m}}'' \ll \mu_b(t_{\mathrm{m}})Q^2$ for $|t - t_m| \ll \tau_F$. Both approaches give $\Omega_F^2\mu_b^2 s_{\mathrm{m}}'' = \Delta\ddot{U}_{\mathrm{m}}$, where μ_b and $\Delta\ddot{U}_{\mathrm{m}} \equiv \partial_t^2\Delta U$ are calculated for $t = t_{\mathrm{m}}$.

The form of $j(q,t)$ depends on the parameter $\Omega_F^2 s_{\mathrm{m}}''/D$. When it is small, the term $\propto p_{\mathrm{opt}}^{-2}$ in $\mathcal{E}_b(t)$ [Eq. (12)] and $z(t)$ is also small away from the diffusion region around q_b. Then $z = 2\pi D\sigma_a^2(t_{\mathrm{m}})$. The pulses of $j(q,t)$ are Gaussian,

$$j(q,t) = \frac{|\mu_a\mu_b|^{1/2}}{2\pi} e^{-R/D} \sum_k e^{-(t-t_k)^2 \Delta\ddot{U}_{\mathrm{m}}/2D} \tag{15}$$

$[\mu_{a,b} \equiv \mu_{a,b}(t_{\mathrm{m}})]$. They are centered at $t_k = t_{\mathrm{m}} + k\tau_F$, with $k = 0, \pm1, \ldots$ [we disregard the delay $\sim \mu_b^{-1}\ln(Q/l_D)$ in t_k]. Eq. (15) corresponds to the fully adiabatic picture, where the escape rate is given by the instantaneous barrier height $\Delta U(t)$.

5.2. Nonadiabatic regime

The current pulses have a different form for $\Omega_F^2 s_{\mathrm{m}}''/D \gg 1$. Because $p_{\mathrm{opt}}^{-2}(t) \propto \kappa_b^2(t,t')$ exponentially increases in time near q_b, the term $\propto p_{\mathrm{opt}}^{-2}$ in $\mathcal{E}_b$ and z becomes dominating before the MPEP reaches the diffusion region $|Q| \sim l_D$. Then Eqs. (7), (12) give

$$j(q,t) = \frac{\mu_b(t)\tilde{\mathcal{E}} D^{1/2}}{\Omega_F\sqrt{s_{\mathrm{m}}''}} e^{-R/D} \sum_{k=-\infty}^{\infty} x_k e^{-x_k}, \tag{16}$$
$$x_k = x_0 \exp(2\pi k/\Omega_F), \qquad x_0 = p_{\mathrm{opt}}(t)Q/D.$$

Note that here $p_{\mathrm{opt}}(t)$ can be smaller than $l_D/\sigma_b^2(t)$.

Eq. (16) does not require the adiabatic approximation, even though its range of applicability overlaps with the range of adiabatic modulation $\Omega_F \ll 1$. The form of the current pulses (16) is totally different from that of the diffusion current $-D\partial_Q\rho$ on the basin boundary $Q = 0$, which was studied by Maier and Stein[14] and Lehmann et $al.$[13] This current is given by Eqs. (5), (12). The regime $\Omega_F^2 s_{\mathrm{m}}''/D \ll 1$, where the current has the form (15), cannot be studied in the approximation[13] at all. The ratio $\tilde{\mathcal{E}}/\sqrt{s_{\mathrm{m}}''} = \Omega_F z_2^{-1/2}$ can be obtained by solving Eq. (13).

For $\Omega_F \ll 1$ the current (16) is a series of distinct strongly asymmetric peaks, with $x_k \approx \exp[-(t - k\tau_F - t_{\mathrm{m}})\mu_b(t_{\mathrm{m}})]$ near the maximum. The transition between the pulse shapes (15) and (16) occurs for $\Omega_F^2 s_{\mathrm{m}}''/D \sim 1$. It is described by Eq. (7) with $\mathcal{E} = (2\pi)^{-1}D^{-1/2}|\mu_a/\mu_b|^{1/2}\exp[-(R - s_{\mathrm{m}})/D]$. We note that, for $\Omega_F \ll 1$, the shape of current pulses in the whole range (14) is the same as for weak modulation,[20] but the parameters depend on A, ω_F differently.

With increasing Ω_F the peaks of j (16) are smeared out and the escape synchronization is weakened. For $\Omega_F \gg 1$ it disappears (s_{m}'' rapidly decreases with ω_F for large Ω_F).

6. PERIOD-AVERAGED ESCAPE RATE

In the range $s_{\mathrm{m}}'' \sim |s_{\mathrm{m}}| \gg D$, the period-averaged escape rate (9) is

$$\overline{W} = \nu \exp(-R/D), \qquad \nu = \bar{\mu}_b\tilde{\mathcal{E}} D^{1/2}/2\pi\sqrt{s_{\mathrm{m}}''}. \tag{17}$$

The prefactor ν can be expressed in terms of z_2. Formally, the result has the same form as the expression[13] obtained before. However, Eq. (17) applies for $|s_{\mathrm{m}}| \gg D$ even where the theory[13] does not apply.

The asymptotic technique developed in this paper allows obtaining the prefactor ν in several limiting cases. For comparatively weak modulation, $D \ll |s_{\mathrm{m}}| \ll R$, Eqs. (13), (17) give the same result as in the method[12] for moderately weak driving. Since the theory for moderately weak driving[12] covers the whole range $|s_{\mathrm{m}}| \ll R$, a transition from the Kramers limit of no modulation to the case of arbitrarily strong modulation is now fully described.

In the whole range where the adiabatic approximation applies, $\Omega_F \ll 1$, we obtain

$$\nu = (2\pi)^{-3/2}|\mu_a\mu_b|^{1/2}D^{1/2}\omega_F(\Delta\ddot{U}_{\mathrm{m}})^{-1/2} \tag{18}$$

where $\mu_{a,b}$ are calculated for $t = t_{\mathrm{m}}$. Interestingly, ν (18) is independent of the modulation frequency.

6.1. Scaling near the bifurcation point

Close to the bifurcational value of the modulation amplitude $A = A_c$ where the metastable and unstable states $q_{a,b}(t)$ merge, the escape rate displays system-independent features. As shown earlier,[25] the activation energy R of the system scales as $R \propto \eta^\xi$, where $\eta \propto (A_c - A)$ is the distance to the bifurcation point along the amplitude axis. Three scaling regimes have been identified for R. With increasing modulation frequency ω_F or decreasing η, the critical exponent ξ changes from $\xi = 3/2$ for stationary systems (adiabatic scaling) to $\xi = 2$ (locally nonadiabatic scaling) and then back to $\xi = 3/2$ (high-frequency scaling). Below we discuss scaling of the prefactor ν in the three regimes.

We start the analysis with the limiting case of slow modulation, $\omega_F t_r \ll 1$. In this case the adiabatic stable and unstable states $q_{a,b}^{\mathrm{ad}}(t)$ are given by the equation $K(q_{a,b}^{\mathrm{ad}}(t), t) = 0$. The adiabatic critical amplitude A_c^{ad} is determined by the condition that the states $q_{a,b}^{\mathrm{ad}}(t)$ touch each other. This happens once per period, and we set $t = k\tau_F$ $(k = 0, \pm 1, \dots)$ at this time moment. We also set $q_{a,b}^{\mathrm{ad}}(k\tau_F) = 0$ for $A = A_c^{\mathrm{ad}}$. Expanding the Langevin equation of motion around this point, we obtain

$$\dot{q} = \alpha q^2 + \beta \delta A^{\mathrm{ad}} - \alpha \gamma^2 (\omega_F t)^2 + f(t), \tag{19}$$

where $\alpha = (1/2)\partial_q^2 K$, $\beta = \partial_A K$, $\gamma^2 = -(2\alpha \omega_F^2)^{-1}\partial_t^2 K$. Here all derivatives are evaluated at $q = t = 0$, $A = A_c^{\mathrm{ad}}$; γ is independent of ω_F; it is assumed (without loss of generality) that $\alpha > 0$; $\delta A^{\mathrm{ad}} = A - A_c^{\mathrm{ad}}$. The force $f(t)$ is a zero-mean white Gaussian noise, $\langle f(t)f(t') \rangle = 2D\delta(t - t')$.

The adiabatic approximation applies provided not only $t_r^{\mathrm{ad}}\omega_F \ll 1$, but also $\partial_t t_r^{\mathrm{ad}} \ll 1$, where $t_r^{\mathrm{ad}}(t) = (1/2)[(\alpha\gamma\omega_F t)^2 - \alpha\beta\delta A^{\mathrm{ad}}]^{-1/2}$ is the adiabatic relaxation time. The relaxation time strongly depends on t and diverges for $A \to A_c^{\mathrm{ad}}$ and $t \to 0$. The inequality $\partial_t t_r^{\mathrm{ad}} \ll 1$ is therefore the most restrictive condition on adiabaticity; it requires that $t_r^{\mathrm{ad}} \ll t_l$, where $t_l = (\alpha\gamma\omega_F)^{-1/2}$ is a new dynamical time scale.

Sufficiently far from A_c^{ad} where the adiabatic approximation still applies (i.e. $t_r^{\mathrm{ad}} \ll t_l$, or, equivalently, $\omega_F \ll |\beta\delta A^{\mathrm{ad}}|/\gamma$), Eq. (18) is simplified. In the adiabatic regime[21–26] the barrier is $\Delta U(t) \propto [|\delta A^{\mathrm{ad}}| + a_c \omega_F^2 (t - t_m)^2]^{3/2}$ (here $a_c \sim A_c^{\mathrm{ad}}$), and $|\mu_{a,b}| \propto |\delta A^{\mathrm{ad}}|^{1/2}$. Then, from Eq. (18), the prefactor in the adiabatic limit scales as $\nu \propto |\delta A^{\mathrm{ad}}|^{1/4}$.

The critical slowing down of the system motion makes the adiabatic approximation inapplicable in the region $|\delta A^{\mathrm{ad}}|/A_c^{\mathrm{ad}} \lesssim \Omega_F$, where the condition $t_r^{\mathrm{ad}} \ll t_l$ is violated. In this range we rewrite Eq. (19) in the form[25]

$$\dot{Q} = Q^2 - \tau^2 + 1 - \eta + \tilde{f}(\tau), \tag{20}$$

where $Q = \alpha t_l q$, $\tau = t/t_l$, $\dot{Q} = dQ/d\tau$, $\tilde{f}(\tau) = (\gamma\omega_F)^{-1}f(t_l\tau)$. The control parameter

$$\eta = \beta(\gamma\omega_F)^{-1}(A_c - A), \qquad A_c \approx A^{\mathrm{ad}} + \gamma\omega_F/\beta, \tag{21}$$

is the distance to the true bifurcation point A_c, which is shifted from A_c^{ad} because of the slowing down of the system and the associated with it delayed response. For small driving frequencies, $\omega_F t_r \ll 1$, where the local expansions (19), (20) apply, the shift in the bifurcational amplitude is linear in frequency, as seen from Eq. (21).

The adiabatic approximation applies for $\eta \gg 1$, leading to $R \propto (\eta-1)^{3/2}$. In contrast, for $\eta \lesssim 1$ the activation energy scales[25] as $R \propto \eta^2$. In this region the most probable escape path $Q_{\mathrm{opt}}(\tau)$, $P_{\mathrm{opt}}(\tau)$ corresponding to Eq. (20) is given by[25]

$$Q_{\mathrm{opt}}(\tau) = \tau - \eta \int_0^\tau d\tau_1 \left[1 - \sqrt{2}e^{-\tau_1^2}\right] e^{\tau^2 - \tau_1^2}, \quad P_{\mathrm{opt}}(\tau) = \eta e^{-\tau^2}/\sqrt{2}. \tag{22}$$

Using these expressions in Eq. (13), we obtain

$$z(\tau) = 4\pi\tilde{D} \int_{-\infty}^\tau d\tau_1 \exp(2\tau^2 - 2\tau_1^2). \tag{23}$$

Here $\tilde{D} = \alpha^{1/2}(\gamma\omega_F)^{-3/2}D$ is the noise intensity corresponding to the scaled force $\tilde{f}(\tau)$. This gives

$$\nu = \nu_0 D^{1/2}|\delta A|^{-1}\omega_F^{5/4}, \qquad \delta A = A - A_c, \tag{24}$$
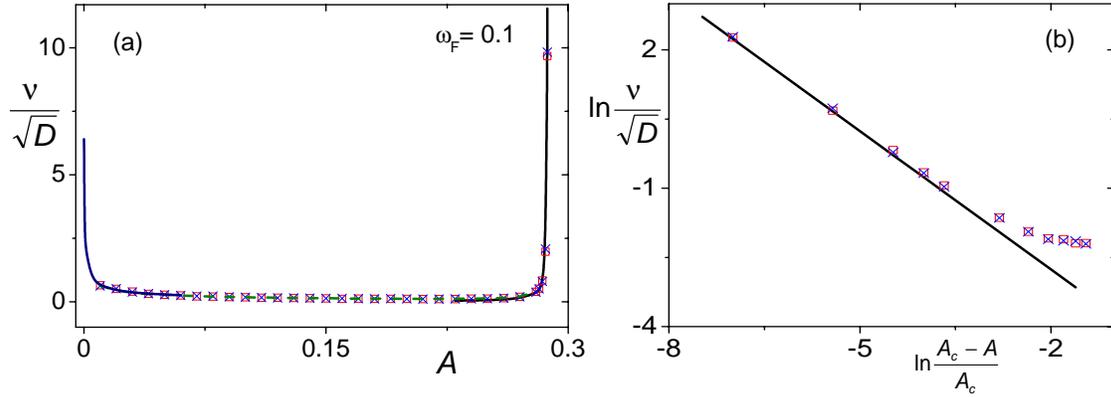
Figure 1. The prefactor ν in the average escape rate $\overline{W}$ (17). The results refer to a Brownian particle with $K(q,t) = q^2 - 1/4 + A\cos(\omega_F t)$, $\omega_F = 0.1$, and describe escape in the regime of strong synchronization, where $\nu \propto D^{1/2}$. In panel (a), the solid line for small A shows the scaling $\nu \propto A^{-1/2}$.[12] In panels (a) and (b), the solid lines for small $\delta A = A - A_c$ show the scaling (24). The dashed line in panel (a) shows the result of the numerical solution of Eq. (13). The squares and crosses show the results of Monte Carlo simulations for $R/D = 5$ and $R/D = 6$, respectively.

where $\nu_0 = (64\pi^7\omega_F)^{-1/4}|\partial_t^2 K\,\partial_q^2 K|^{1/8}/|\partial_A K|$.

From Eq. (24), the prefactor $\nu \propto |\delta A|^{-1}$ sharply increases as the modulation amplitude approaches A_c. This is qualitatively different from the decrease of ν in the adiabatic approximation. The result agrees with the numerical solution of Eqs. (13), (17) for a model system shown in Fig. 1. The calculations in a broad range of A are also confirmed by Monte Carlo simulations.

For high frequencies, $\Omega_F \gg 1$, escape is not synchronized by the modulation. The prefactor in the escape rate is $\nu = |\bar{\mu}_a\bar{\mu}_b|^{1/2}/2\pi$, it is independent of the noise intensity D. Near the bifurcation point it scales as in stationary systems,[21, 22] where $\nu \propto |\delta A|^{1/2}$ and $R \propto |\delta A|^{3/2}$. We note that very close to the bifurcation point modulation is necessarily fast, because $|\bar{\mu}_{a,b}| \to 0$ for $A \to A_c$. Therefore the prefactor always goes to zero for $A \to A_c$. However, for small ω_F the corresponding region of δA is exponentially narrow.[25]

7. RESULTS FOR A MODEL SYSTEM

To illustrate the findings, we consider a simple model system of a Brownian particle in a cubic potential subject to sinusoidal modulation. The equation of motion is of the form

$$\dot{q} = K(q,t) + f(t), \quad K = q^2 - 1/4 + A\cos(\omega_F t). \tag{25}$$

7.1. The adiabatic regime

The adiabatic stable and unstable states of the system (25) are

$$q_{a,b}^{\mathrm{ad}}(t) = \mp\left[1/4 - A\cos(\omega_F t)\right]^{1/2}, \tag{26}$$

and the adiabatic critical amplitude is $A_c^{\mathrm{ad}} = 1/4$. The adiabatic barrier height is

$$\Delta U(t) = (4/3)\left[1/4 - A\cos(\omega_F t)\right]^{3/2}. \tag{27}$$

Its minimum $\Delta U_{\mathrm{m}} = (4/3)(1/4 - A)^{3/2}$ is reached for $t_{\mathrm{m}} = k\tau_F$ (here and below $k = 0, \pm 1, \ldots$). The adiabatic optimal escape trajectories are centered around t_{m} and have the form

$$q_{\mathrm{opt}}^{\mathrm{ad}}(t) = (1/4 - A)^{1/2}\tanh\left[(1/4 - A)^{1/2}t\right]. \tag{28}$$

The adiabatic relaxation rates are

$$\mu_{a,b}(t_{\mathrm{m}}) = \mp 2(1/4 - A)^{1/2}. \tag{29}$$

The reduced curvature $\Omega_F^2 s_{\mathrm{m}}''$ of the function $s(\phi)$ in the boundary-layer distribution at $\phi_{\mathrm{m}} = \omega_F t_{\mathrm{m}}$ is given by $\mu_b^{-2}(t_{\mathrm{m}})\Delta \ddot{U}_{\mathrm{m}}$, which becomes

$$\Omega_F^2 s_{\mathrm{m}}'' = (1/2)A\omega_F^2(1/4 - A)^{-1/2}. \tag{30}$$

Therefore the condition (14) of strong but slow modulation, which must hold for the pulses of the escape current to be of Gaussian shape, takes the form

$$\omega_F^2 \ll (8/3)(1/4 - A)^2/A. \tag{31}$$

It becomes more and more restrictive for the modulation frequency as the modulation amplitude A approaches the adiabatic bifurcational value $1/4$.

The prefactor ν of the period-averaged escape rate in the adiabatic limit for sufficiently strong modulation is given by Eq. (18). For our model it has a simple explicit form

$$\nu = (2\pi^{3/2})^{-1}D^{1/2}(1/4 - A)^{1/4}A^{-1/2}. \tag{32}$$

As expected, $\nu \propto A^{-1/2}$ for small amplitude, whereas close to the adiabatic bifurcation point $\nu \propto (A_c^{\mathrm{ad}} - A)^{1/4}$.

7.2. Locally nonadiabatic regime

As explained in Section 6, sufficiently close to the bifurcation point the adiabatic approximation breaks down. As a result, the bifurcation point A_c shifts away from A_c^{ad} (to higher amplitude, in our case). Close to A_c the pulses of escape current become strongly asymmetric, even though the modulation frequency is small. The scaling of the prefactor in the period-averaged escape rate also changes dramatically, from decreasing (as in the adiabatic approximation) to increasing for $A \to A_c$. From Eq. (24)

$$\nu = (64\sqrt{2}\pi^7)^{-1/4}D^{1/2}|\delta A|^{-1}\omega_F^{5/4}. \tag{33}$$

The results on the prefactor for the discussed model system are shown in Figure 1. They refer to the modulation frequency $\omega_F = 0.1$ (the relaxation time in the absence of modulation is $t_{\mathrm{r}}^{(0)} = 1/2$). The dependence of $\nu/\sqrt{D}$ on the modulation amplitude A is shown in panel (a). The solid line for small A represents Eq. (32), which also agrees with the results[12] for moderately weak modulation. The solid line close to the bifurcational amplitude $A_c \simeq 0.29$ is given by Eq. (33). The dashed line for intermediate values of A is given by Eq. (17) with $\tilde{\mathcal{E}}/\sqrt{s_{\mathrm{m}}''}$ evaluated by numerically integrating Eq. (13). The analytical results agree with the results of simulations represented by squares and crosses. Panel (b) shows in more detail the locally nonadiabatic scaling $\nu \propto |\delta A|^{-1}$ in the region near A_c.

The simulations have been done using the standard second-order integration scheme[27] for stochastic differential equations. The period-averaged escape rate was found as a reciprocal of the average dwell time of particles leaving the attraction basin. For each set of parameter values we accumulated $\sim 10^5$ escape events. The prefactor of the escape rate ν was evaluated as $\nu = \overline{W}\exp(R/D)$. The values of activation energy R were obtained independently by solving the appropriate instantonic problem. We checked previously[28] that these value agree extremely well with Monte Carlo simulations. For each value of A the noise intensity D was adjusted so as to keep R/D fixed at $R/D = 5$ (squares) and $R/D = 6$ (crosses).

8. CONCLUSIONS

The results of this paper and the previous work allow us to draw the general scheme of the dependence of the rate of activated escape on the modulation parameters. This scheme is sketched in Fig. 2.

The range of low modulation amplitude corresponds to the case where the modulation-induced change of the activation energy of escape $|s_{\mathrm{m}}|$ is small compared to the noise intensity D. In this case the major effect of
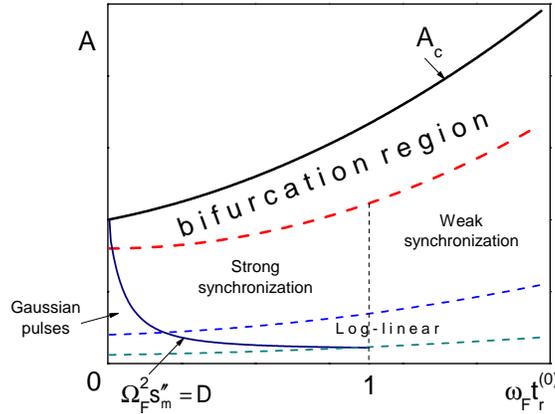
Figure 2. Different regions of escape behavior in modulated overdamped systems depending on the modulation frequency ω_F and amplitude A; $t_r^{(0)}$ is the relaxation time in the absence of modulation.

modulation is effective heating of the system (which depends on energy, for underdamped systems[7, 29]). Escape is not synchronized in this regime.

Synchronization first emerges for stronger driving, where $|s_m| \gg D$. Here there is a broad range of modulation amplitudes where the activation energy change is linear in the amplitude, $|s_m| \propto A$. Strong synchronization occurs for small frequencies,[12] where $\omega_F t_r^{(0)} \ll 1$. Here, the escape current has peaks with width much smaller than the modulation period. The prefactor in the period-averaged escape rate scales as $(D/A)^{1/2}$. For high frequencies $|s_m|$ exponentially decays with ω_F.

The synchronization persists for higher modulation amplitudes. The shape of the peaks of escape current is Gaussian for $\Omega_F^2 |s_m| \ll D$ and is strongly asymmetric and non-Gaussian for higher frequencies. For very high modulation frequencies exponentially strong synchronization of escape disappears. The escape current is still modulated in time, of course, but it does not have a shape of sharp narrow peaks even for small noise intensity.

Of special interest is the bifurcation region. Here the adiabaticity is broken. For small modulation frequencies the escape current has the form of strongly asymmetric narrow peaks. The activation energy of escape scales with the distance to the bifurcation amplitude A_c as $(A_c - A)^2$, whereas the prefactor in the period-averaged escape rate is $\propto (A_c - A)^{-1}$.

In conclusion, we have obtained a general solution of the problem of noise-induced escape in periodically modulated overdamped systems. With increasing modulation frequency, the pulses of escape current change from Gaussian to strongly asymmetric; for large ω_F current modulation is smeared out. The prefactor ν in the period-averaged escape rate is a strongly nonmonotonic function of the modulation amplitude A for low frequencies. It first drops with increasing A to $\nu \propto (D/A)^{1/2}$,[12] then varies with A smoothly,[13, 14] and then sharply increases, $\nu \propto D^{1/2}/(A_c - A)$ near the bifurcation amplitude A_c. We found three scaling regimes near A_c, where $\nu \propto (A_c - A)^\zeta$ with $\zeta = 1/4, -1,$ or $1/2$. The widths of the corresponding scaling ranges strongly depend on the modulation frequency.

REFERENCES

1. W. Wernsdorfer, E.B. Orozco, K. Hasselbach, A. Benoit, B. Barbara, N. Demoncy, A. Loiseau, H. Pascard, and D. Mailly, Phys. Rev. Lett. **78**, 1791 (1997); W.T. Coffey, D.S.F. Crothers, J.L. Dormann, Yu.P. Kalmykov, E.C. Kennedy, and W. Wernsdorfer, Phys. Rev. Lett. **80**, 5655 (1998).

2. R.H. Koch, G. Grinstein, G.A. Keefe, Yu Lu, P.L. Trouilloud, and W.J. Gallagher, Phys. Rev. Lett. **84**, 5419 (2000).

3. E. B. Myers, F. J. Albert, J. C. Sankey, E. Bonet, R. A. Buhrman, and D. C. Ralph, Phys. Rev. Lett. **89**, 196801 (2002).

4. Y. Yu and S. Han, Phys. Rev. Lett. **91**, 127003 (2003).

5. A. Wallraff, A. Lukashenko, J. Lisenfeld, A. Kemp, M. V. Fistul, Y. Koval, and A. V. Ustinov, Nature **425**, 155 (2003).

6. I. Siddiqi, R. Vijay, F. Pierre, C. M. Wilson, M. Metcalfe, C. Rigetti, L. Frunzio, and M. H. Devoret, Phys. Rev. Lett. **93**, 207002 (2004).

7. M.H. Devoret, D. Esteve, J.M. Martinis, A. Cleland, and J. Clarke, Phys. Rev. B **36**, 58 (1987). E. Turlot, S. Linkwitz, D. Esteve, C. Urbina, M.H. Devoret, and H. Grabert, Chem. Phys. **235**, 47 (1998).

8. J. S. Aldridge and A. N. Cleland, cond-mat/0406528 (2004).

9. For a recent review see S.M. Soskin, R. Mannella, and P.V.E. McClintock, Phys. Rep. **373**, 247 (2003).

10. See also M.I. Dykman and D. Ryvkine, Phys. Rev. Lett. **94**, 070602 (2005).

11. H. Kramers, Physica (Utrecht) **7**, 240 (1940).

12. V.N. Smelyanskiy, M.I. Dykman, and B. Golding, Phys. Rev. Lett. **82**, 3193 (1999).

13. J. Lehmann, P. Reimann, and P. Hänggi, Phys. Rev. Lett. **84**, 1639 (2000); Phys. Rev. E **62**, 6282 (2000).

14. R.S. Maier and D.L. Stein, Phys. Rev. Lett. **86**, 3942 (2001).

15. R. Graham and T. Tél, Phys. Rev. Lett. **52**, 9 (1984); J. Stat. Phys. **35**, 729 (1984); Phys. Rev. A **31**, 1109 (1985).

16. M.V. Berry, Adv. Phys., **35**, 1 (1976).

17. D. Ludwig, SIAM Rev. **17**, 605 (1975).

18. M.I. Freidlin and A.D. Wentzell, *Random Perturbations in Dynamical Systems*, 2nd ed. (Springer Verlag, NY 1998).

19. D. Ryter and P. Jordan, Phys. Lett. **104A**, 193 (1984).

20. V.N. Smelyanskiy, M.I. Dykman, H. Rabitz, B.E. Vugmeister, S.L. Bernasek, and A.B. Bocarsly, J. Chem. Phys. **110**, 11488 (1999).

21. J. Kurkijärvi, Phys. Rev. B **6**, 832 (1972).

22. M.I. Dykman and M.A. Krivoglaz, Physica **104A**, 480 (1980).

23. R.H. Victora, Phys. Rev. Lett. **63**, 457 (1989).

24. O.A. Tretiakov, T. Gramerspacher, and K.A. Matveev, Phys. Rev. B **67**, 073303 (2003); O.A. Tretiakov and K.A. Matveev, cond-mat/0411075.

25. M.I. Dykman, B. Golding, and D. Ryvkine, Phys. Rev. Lett. **92**, 080602 (2004).

26. M. Bier, Phys. Rev. E **71**, 011108 (2005).

27. R. Mannella, Intern. J. Mod. Phys. C **13**, 1177 (2002).

28. D. Ryvkine, M.I. Dykman, and B. Golding, Phys. Rev. E **69**, 061102 (2004).

29. A.I. Larkin and Yu.N. Ovchinnikov, J. Low Temp. Phys. **63**, 317 (1986); B.I. Ivlev and V.I. Mel'nikov, Phys. Lett. A **116**, 427 (1986); S. Linkwitz and H. Grabert, Phys. Rev. B **44** 11888, 11901 (1991).